Witos, Joanna; Karjalainen, Erno; Tenhu, Heikki; Wiedmer, Susanne K.

CE and asymmetrical flow-field flow fractionation studies of polymer interactions with surfaces and solutes reveal conformation changes of polymers

RESEARCH ARTICLE

CE and asymmetrical flow-field flow fractionation studies of polymer interactions with surfaces and solutes reveal conformation changes of polymers

Joanna Witos[1,2] ⬤ | Erno Karjalainen[1] ⬤ | Heikki Tenhu[1] ⬤ | Susanne K. Wiedmer[1] ⬤

[1]Department of Chemistry, University of Helsinki, Helsinki, Finland

[2]Department of Bioproducts and Biosystems, Aalto University, Espoo, Finland

Correspondence
Dr. Susanne K. Wiedmer, Department of Chemistry, A.I. Virtasen aukio 1, P.O. Box 55, FIN-00014 University of Helsinki, Finland.
Email: susanne.wiedmer@helsinki.fi

Funding information
Magnus Ehrnrooth Foundation; Academy of Finland, Grant/Award Numbers: 266342, 307475

Amphiphilic diblock copolymers consisting of a hydrophobic core containing a polymerized ionic liquid and an outer shell composed of poly(*N*-isoprolylacrylamide) were investigated by capillary electrophoresis and asymmetrical flow-field flow fractionation. The polymerized ionic liquid comprised poly(2-(1-butylimidazolium-3-yl)ethyl methacrylate tetrafluoroborate) with a constant block length ($n = 24$), while the length of the poly(*N*-isoprolylacrylamide) block varied ($n = 14$; 26; 59; 88). Possible adsorption of the block copolymer on the fused silica capillary, due to alterations in the polymeric conformation upon a change in the temperature (25 and 45 °C), was initially studied. For comparison, the effect of temperature on the copolymer conformation/hydrodynamic size was determined with the aid of asymmetrical flow-field flow fractionation and light scattering. To get more information about the hydrophilic/hydrophobic properties of the synthesized block copolymers, they were used as a pseudostationary phase in electrokinetic chromatography for the separation of some model compounds, that is, benzoates and steroids. Of particular interest was to find out whether a change in the length or concentration of the poly(*N*-isoprolylacrylamide) block would affect the separation of the model compounds. Overall, our results show that capillary electrophoresis and asymmetrical flow-field flow fractionation are suitable methods for characterizing conformational changes of such diblock copolymers.

KEYWORDS

asymmetrical flow-field flow fractionation, capillary electrophoresis, poly(*N*-isoprolylacrylamide), polymerized ionic liquids, thermoresponsive polymers

1 | INTRODUCTION

Responsive polymers are defined as macromolecular compounds that can undergo changes in their properties by adjusting the chemical or physical conditions of their surrounding, for example, by changes in pH, pressure, temperature, solvent composition, ionic strength, light, and electric and magnetic fields [1,2]. One of the most studied temperature-responsive

---

polymers is poly(*N*-isoprolylacrylamide) (PNIPAM) [3]. The phase transition temperature of PNIPAM in aqueous solution is around 32 °C [4], meaning that the polymer will be insoluble in water above that temperature. Over the last few years, much attention has been paid toward the usability of polymeric structures for biosensors, as support of catalysts, and for drug encapsulation [5–11]. In this work, conformational changes of amphiphilic diblock copolymers consisting of a hydrophobic block of a polymerized ionic liquid (PIL) and composed hydrophilic one of PNIPAM were studied. In water the polymers are capable to build up micelles and they in general have a tendency to aggregate.

Ionic liquids (ILs) are organic salts composed entirely of ions that are in a liquid state at temperatures below 100 °C [12]. They are chemically and thermally stable, exhibit low flammability and low vapor pressure, decreasing their release to the atmosphere. Due to their physicochemical properties and their usability in a broad range of applications, they have become an essential area of research in organic synthesis, in various industrial processes, and in separation of biologically relevant compounds [13–17]. ILs that contain a polymerizable double bond can be polymerized to PILs [18]. Mostly, they are polycations with low molar mass counter ions, which can be utilized in liquid–liquid phase separations and gas separation membranes [19–21]. In addition, they are used as dynamic or semi-permanent coatings in CE or as additives in the BGE for CE [2,22–26].

Our goal was to demonstrate the suitability of combining the results of two complementary separation techniques, that is, CE and asymmetrical field flow field fractionation (AF4), for the characterization of diblock copolymers. The series of amphiphilic diblock copolymers that we investigated, comprised of a hydrophobic PIL block with a constant length and PNIPAM block with varying degree of polymerization, that is, PIL_{24}–$PNIPAM_{14}$, PIL_{24}–$PNIPAM_{26}$, PIL_{24}–$PNIPAM_{59}$, and PIL_{24}–$PNIPAM_{88}$ (Figure 1). Changes in the electrophoretic mobilities of the copolymers, due to changes in the polymeric micelle formation above and below the phase transition temperature, were monitored by CE at room and elevated temperature. To compare and evaluate the effect of temperature on the polymeric micelle formation, AF4 was applied as well. AF4 is a useful technique for the separation and characterization of high-molar mass polymers and particles, providing direct information on particle size, molar mass, and diffusion coefficients. We have previously successfully utilized AF4 in studies on liposomes, lipoproteins, nanoparticles, and polymers [27–30].

To gain information on the solute–polymer interaction of the amphiphilic diblock copolymers, further studies were carried out using EKC. The methodology is widely used for the separation of both neutral and charged compounds, and typically, anionic additives are employed as the pseudostationary phase. In case of positively charged additives,
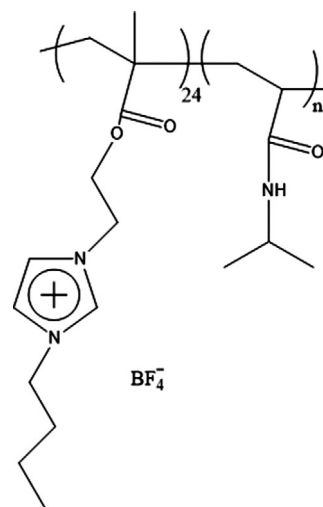

FIGURE 1 Structures of diblock copolymers where *n* is 14; 26; 59; or 88

the additives will adsorb onto the fused silica capillary, resulting in a reversed EOF. If a structural reorganization of the PIL–PNIPAM diblock copolymer takes place upon a change in the temperature, then the surface charge of the copolymer micelle will change as well and this will strongly affect the EOF. Therefore, the EOF was first studied using one preselected block copolymer (PIL_{24}–$PNIPAM_{59}$). The series of diblock copolymers selected for this study were used as pseudostationary phase for the separation of some neutral model compounds, that is, nonpolar alkyl benzoates and steroids. The aim was to find out whether a possible change in the structure of the block copolymer, due a change in the temperature, has an effect on the separation of the neutral model compounds. Our results demonstrate that the combination of these two complementary techniques (CE and AF4) is valuable when information about the hydrophobicity of diblock polymers is required. The results were compared to light scattering and zeta potential studies and it was shown that the changes in chemical composition, added salts, and temperature cause profound changes in the aggregate structure. These changes were reflected in the CE and AF4 results as well.

2 | MATERIALS AND METHODS

2.1 | Materials

Thiourea, methyl benzoate, ethyl benzoate, propyl benzoate, pentyl benzoate, hexyl benzoate, BSA, sodium azide, testosterone, progesterone, and hydrogen sodium phosphate were purchased from Sigma (Darmstadt, Germany). Dihydrogen sodium phosphate monohydrate and methanol (HPLC-grade) were obtained from Mallinckrodt Baker (Deventer, The Netherlands). Sodium azide was purchased from VWR (Leuven, Belgium). Sodium hydroxide (1 M) was from

FF-Chemicals (Yli-Ii, Finland). pH solutions (7 and 10) used for calibrating the pH meter were purchased from Merck (Darmstadt, Germany). The synthesis and characterization of the studied diblock copolymers have been reported previously [18].

2.2 | Instrumentations and methods

The CE experiments were carried out with a Hewlett Packard Chemstation ^{3D}CE system equipped with a diode-array detector (detection at 200, 214, 238, and 254 nm) and an air-cooling device for the capillary cassette. The temperature of the autosampler was controlled with MGW Lauda M3 water bath (Lauda-Königshofen, Germany), and the measurements were done at 25 and 45 °C. Uncoated fused silica capillaries were from Polymicro Technologies (Phoenix, AZ, USA). Dimensions were 50 μm id and 375 μm od. The length of the capillary to the detector (L_{det}) was 40.0 cm and the total length (L_{tot}) was 48.5 cm. Uncoated fused silica capillary was pretreated by flushing for 20 min with 1 M NaOH, 10 min with 0.1 M NaOH, 25 min with MQ water, and 5 min with sodium phosphate buffer at a pressure of 940 mbar. The CE separation conditions were as follows: the voltage was ±25 kV and the sample injection was for 3 s at 50 mbar. Before each run, the capillary was rinsed for 2 min with sodium phosphate buffer (ionic strength of 20 mM and pH of 7.4). The electrophoretic runs were repeated three to five times.

An Eclipse AF4 separation system (Wyatt Europe, Dernbach, Germany) combined with an isocratic pump and degasser (Agilent 1100 series, Agilent Technology, Böblingen, Germany), multiangle laser light scattering detector (DAWN HELEOS II MALLS; Wyatt Europe), and a refractive index detector (Optilab rEX; Wyatt Europe) was used to analyze the diblock copolymers. The temperature of the separation channel was controlled by Thermos (Wyatt Europe). The separation membrane was a regenerated cellulose membrane with a molecular mass cutoff of 10 kDa (Superon, Dernbach, Germany). A total of 20 mM sodium phosphate buffer preserved with 0.02% m/v sodium azide was filtered through a membrane with a pore size of 0.1 μm (VVLP, Merck Millipore, Cork, Ireland) and used as a carrier liquid. The separation membrane was conditioned with 1 mg/mL BSA (diluted in carrier solution) according to the following procedure: the detector flow rate was set to 1.0 mL/min, the constant cross flow rate was 3.0 mL/min, and the focusing flow rate was 1.5 mL/min. For analyzing the diblock copolymers, the following conditions were used. The sample volume was 60 μL and the detector flow rate was set at 1.0 mL/min. In focus mode, the injection was fixed at 0.2 mL/min with an injection time of 2 min and the cross-flow rate was 1.7 mL/min. In elution mode, a gradient profile was used and the flow rate conditions were as follows: 1.7 mL/min at 0-10 min; 1.7-0 mL/min at 10-15 min; 0 mL/min at 15-20 min. To flush

the whole system, including the autosampler, the last step of every measurement contained an elution and injection step without cross-flow. All experiments were performed at 25 and 45 °C.

The pH meter was from Mettler Toledo (Columbus, OH, USA). Distilled water was purified with a Millipore water purification system (Millipore, Molsheim, France).

The light scattering measurements at an angle of 173° and the zeta potential measurements were conducted with a Malvern Instrument ZetaSizer Nano-ZS equipped with a 4 mW He-Ne laser operating at 633 nm and using disposable folded capillary cells. The samples were filtered through a poly(vinylidene fluoride) membrane with a pore size of 0.45 μm and degassed under mild vacuum prior to measurements. The sample was stabilized at the starting temperature of 20 °C for 15 min and heated to 60 °C with measurements every 1 °C, stabilizing the sample for 2 min before measuring. Dynamic light scattering (DLS) and zeta potential measurements were performed at each temperature.

2.3 | Buffer and sample preparation

Sodium phosphate buffer was prepared by mixing sodium dihydrogen phosphate and disodium hydrogen phosphate to yield an ionic strength of 20 mM and a pH of 7.4. Before use, the CE buffer solution was filtered through a 0.45-μm syringe filter (Gelman Sciences, Ann Arbor, MI, USA). Thiourea at a concentration of 0.5 mM dissolved in BGE solution was used as a neutral EOF marker. The diblock copolymers were dissolved in dimethylformamide to yield 0.5% m/v polymeric solutions, followed by water addition until a slight turbidity was observed [18]. The polymer solutions were further dialyzed against water at room temperature. To obtain the final concentrations of alkyl benzoates and steroids, the stock solutions were diluted with the running buffer (pH 7.4, ionic strength of 20 mM). All buffer and sample solutions were stored at +4 °C.

The samples for light scattering and zeta potential measurements were prepared by mixing the polymers with the phosphate buffer or with pure water to an approximate concentration of 0.9 mg/mL. If the solutions were visually homogenous, they were transferred into a volumetric flask and diluted to a precise concentration of 0.5 mg/mL. The block copolymer samples were stored refrigerated and were allowed to stabilize at least overnight before any measurements. The PIL homopolymer sample was stored at room temperature and was stabilized for 2 h before measuring.

3 | RESULTS AND DISCUSSION

The amphiphilic diblock copolymers PIL_{24}–$PNIPAM_{14}$, PIL_{24}–$PNIPAM_{26}$, PIL_{24}–$PNIPAM_{59}$, and PIL_{24}–

PNIPAM$_{88}$ were studied by CE and AF4. The block copolymers had a water-insoluble PIL block with a constant degree of polymerization of 24 and PNIPAM chains with different lengths were grown in the original PIL. The subscripts in the names of the copolymers refer to the degrees of polymerization of respective blocks and the general chemical structure of the copolymers is given in Figure 1.

First, the possibility to utilize the studied diblock copolymers as dynamic or semipermanent fused silica capillary coatings in CE was evaluated. Next, the effect of the diblock copolymer composition on the EOF was studied, and the conformational changes observed by CE were further confirmed by AF4. Finally, the hydrophobicity of the diblock copolymeric micelles was characterized by using them as pseudostationary phase in EKC for the separation of low molar mass neutral model analytes.

3.1 | Effect of counterion on the solution properties of the block copolymers

The effect of counterion on the solubility behavior of polycations is known to be strong [31,32]. In this study, the electrophoretic measurements were conducted in 20 mM phosphate buffer and thus it is reasonable to assume that some ion exchange from original tetrafluoroborate ions in the polymer to phosphate present in the buffer will take place. To test this hypothesis, the block copolymers and the PIL homopolymer were mixed both with water and the buffer (see the experimental part for details). It was noticed already during the sample preparation that neither the PIL homopolymer nor the two copolymers with shorter PNIPAM blocks of 14 and 26 repeating units did form a homogenous mixture in pure water, but they did form a visually homogenous solution in the phosphate buffer. This already indicates that the presence of phosphate ions increases the solubility of the PIL block.

The particle distributions of the directly dispersed particles were studied by DLS in order to compare to the particles previously made by careful solvent exchange from DMF to water [18].

The intensity average distribution of particle sizes at 173 ° scattering angle at 20 °C for PIL$_{24}$–PNIPAM$_{88}$ (Supporting Information Figure S1) is broad, whereas the distribution obtained by solvent exchange was narrow and bimodal [18]. For PIL$_{24}$–PNIPAM$_{59}$ (Supporting Information Figure S2), the distribution is strikingly similar to the one obtained by careful solvent exchange from dimethyl formamide to water. PIL$_{24}$–PNIPAM$_{59}$ forms equilibrium particles also by direct dissolution, whereas this is not the case with the longest block copolymer.

The distributions given as intensity distribution emphasizes the relative contribution from larger particles. Thus, it can be seen from the volume average distributions in Supporting Information Figures S1 and S2 that most of the material is
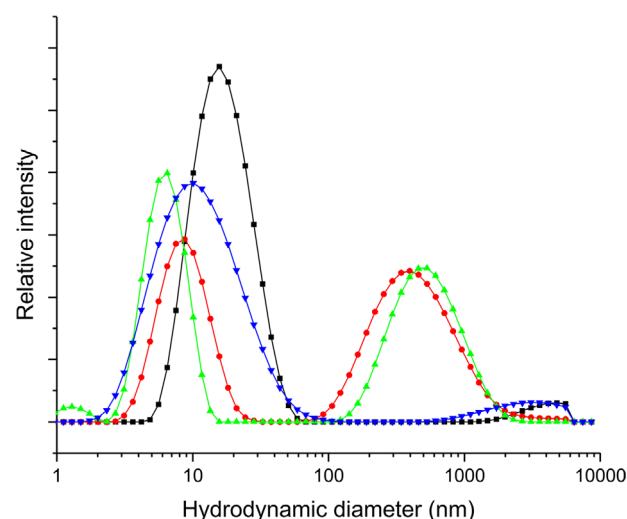

FIGURE 2 Intensity average hydrodynamic diameters of PIL$_{24}$–PNIPAM$_{88}$ (black ■), PIL$_{24}$–PNIPAM$_{59}$ (red ●), PIL$_{24}$–PNIPAM$_{26}$ (green ▲), and PIL$_{24}$–PNIPAM$_{14}$ (blue ▼) in 20 mM phosphate buffer at 20 °C. The scattering angle was 173°

located in much smaller aggregates. This was likely the case also with solvent exchanged aggregates. The reader is advised to note that the volume average distributions have been created from intensity averages by assuming spherical particles, which may not always be valid. When the block copolymers were dissolved in 20 mM phosphate buffer (used as a running buffer in electrophoretic experiments), the size distributions change considerably (Figure 2). As already noted during the sample preparation (see discussion above), the presence of phosphate salt increases the solubility of the block copolymers. Some aggregates are still present in the buffer for the three shortest PNIPAM blocks. This can be observed as large distributions in Figure 2, although majority of the particles formed by PIL$_{24}$–PNIPAM$_{14}$ are too large to be observed by DLS. However, the amount of aggregates is low.

As the buffer is the relevant medium in the framework of this study, the rest of the text will discuss the solution behavior in the buffer, unless otherwise noted.

The PIL block is kept insoluble in water by the interactions between the cationic repeating units and tetrafluoroborate counterions [18]. The block copolymer concentration was 0.5 mg/mL in all cases, which translates to 0.82-1.3 mM BF$_4^-$ concentration, depending on the relative content of PIL units in the block copolymer. For the PIL homopolymer, the counterion concentration was 1.5 mM. Thus, the phosphate ions were present in excess and at least some ion exchange was bound to take place. The excess was naturally significantly higher in the electrophoresis measurements as more buffer is introduced constantly.

The PIL homopolymer has a transition resembling upper critical solution temperature type of transition in the phosphate buffer (Supporting Information Figure S3). The particle

size and the intensity of scattered light both decrease noticeably, although particles clearly exist also at higher temperatures. It has previously been observed that certain ions may induce such behavior for polycations. For this particular polycation, a similar transition takes place at least in a mixture of phosphate and tetrafluoroborate [33,34].

The decrease in particle size can be rationalized by enrichment of phosphate ions on the surface of the formed particles, which makes it possible for the outmost parts to become more soluble with increasing temperature, which in turn decreases the particle size. In this rationalization, most of the tetrafluoroborate ions stay in the bulk of the particle and thus the counterion of the PIL chains gradually changes from phosphate to tetrafluoroborate when going deeper into the particles. The PIL homopolymer displays a nearly constant zeta potential of approximately 27 mV (Supporting Information Figure S4), which means that the colloid is not stabilized by electrostatic interactions alone. Yet the dispersion stays visually stable over time, so other stabilizing interactions must contribute as well.

It can be concluded that the presence of phosphate ions increases the solubility of the PIL block considerably compared to pure water. The ion exchange also affects the phase transition of the PNIPAM block because the increase in the scattering intensity (indicating phase separation in the system) starts at considerably lower temperatures for polymers in phosphate buffer (Supporting Information Figure S5). This can be rationalized by interactions between the blocks. It is known that phosphate salts decrease the phase transition temperature of PNIPAM, but for a 20 mM solution the effect is not significant [35].

An alternative explanation for the lower transition temperature can be presented as well. It is known that hydrophobic end groups decrease the phase transition temperature of PNIPAM unless the molecular mass is high [36,37]. However, if aggregates form and the end groups' contact with water is reduced, no such effect can be observed [38,39]. So it can be rationalized that the presence of phosphate ions exchange the counterion of the PIL block partially, but still enough for the aggregates to break. As the interactions between the repeating units of the PIL block and water stay less favorable than those of the NIPAM repeating units, a decrease in transition temperature is observed.

3.2 | Adsorption of a diblock copolymer on the fused silica capillary wall

The stability of the EOF depends on the constancy of the zeta potential between the fused silica capillary wall and the running buffer solution. Adsorption of analytes, BGE components, and modifiers might result in changes in the zeta potential, causing unstable EOF values. In this work, diblock copolymers were added to the running buffer as BGE modifiers. To investigate whether the diblock copolymers adsorb
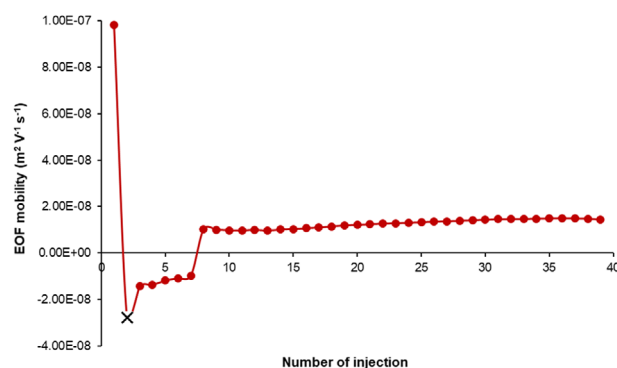

FIGURE 3 Interactions between PIL_{24}–$PNIPAM_{59}$ and the fused silica capillary wall at 45 °C. Indication of the EOF mobility without the copolymer in the BGE solution (red ●); EOF mobility with the copolymer in the BGE solution (black ×). Running conditions: ± 25 kV, injection for 3 s at 50 mbar, sodium phosphate buffer pH 7.4 (ionic strength of 20 mM), L_{tot} 48.5 cm, L_{det} 40 cm, UV-detection at 238 nm, 0.5 mM thiourea as EOF marker. The running time was 15 min. Before each run, the capillary was rinsed with BGE solution for 2 min

onto the fused silica capillary wall and induce major changes in the EOF, the capillary was treated with phosphate buffer (ionic strength of 20 mM) at pH 7.4 containing one of the studied copolymers. The electrophoretic studies were conducted at 25 and 45 °C. The temperatures were chosen from both sides of the PNIPAM lower critical solution temperature (LCST)-type phase transition temperature, which is most often reported to be 32 °C [3]. In this way, the changes induced by the phase transition on structures of the aggregates and their possible effect on the adsorption behavior of the copolymers onto capillary walls could be studied.

First, the EOF marker was introduced into the capillary without addition of copolymer in the BGE solution. The corresponding EOF mobility was $9.81 \cdot 10^{-8}$ m^2/V/s with an RSD of 1.48% ($n = 3$). Subsequent runs with the copolymer in the BGE solution indicated a reversal of the EOF from cathodic to anodic EOF. The EOF mobility decreased to $-2.77 \cdot 10^{-8}$ m^2/V/s, confirming interactions between the copolymer and the fused silica capillary wall. To check whether the interactions are weak or strong, some repetitive runs without addition of copolymer in the BGE solution were carried out. Our results demonstrate that after five runs the EOF turned again to cathodic, which indicates rather weak interactions between the PIL_{24}–$PNIPAM_{59}$ block copolymer and the fused silica capillary wall (Figure 3). After another 15 subsequent injections of the EOF marker, the EOF became stable and the mobility value stabilized at $1.43 \cdot 10^{-8}$ m^2/V/s (RSD 3.88%; $n = 15$). The decrease in the EOF mobility, comparing the first run with the last one (both runs without addition of diblock copolymer in the BGE solution), suggests that PIL_{24}–$PNIPAM_{59}$ adsorbs on the fused silica capillary wall. This was rather expected because of the positive surface charge of the copolymer, however, at this stage we
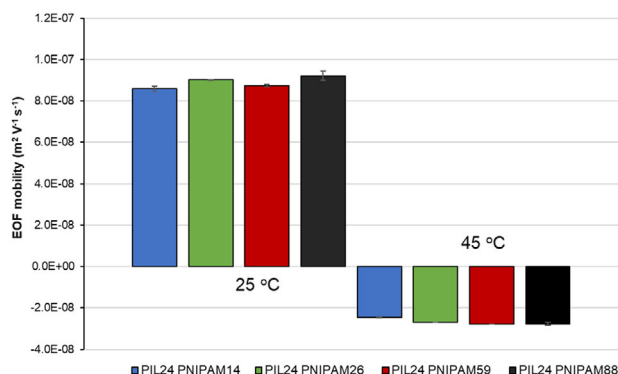
FIGURE 4 Effect of PIL_{24}–$PNIPAM_{(n\,=\,14,\,26,\,50,\,88)}$ block copolymers on EOF mobility at 25 and 45 °C. Running conditions: ±25 kV, injection for 3 s at 50 mbar, sodium phosphate buffer pH 7.4 (ionic strength of 20 mM), L_{tot} 48.5 cm, L_{det} 40 cm, UV-detection at 238 nm, 0.5 mM thiourea as EOF mobility marker. The run time was 6 min. Before each run, the capillary was rinsed with BGE solution for 2 min. The number of runs was 5

cannot differentiate between the type of interactions, that is, electrostatic or hydrophobic, affecting the adsorption of the copolymer onto the negatively charged fused silica capillary. To summarize, the PIL_{24}–$PNIPAM_{59}$ diblock copolymer provided a rather stable semipermanent coating on the capillary wall; however, flushing the capillary with the diblock copolymer solution before each run would guarantee a highly stable semipermanent coating.

3.3 | Effect of diblock copolymer composition on the EOF

The effect of the composition of the diblock copolymer on the EOF was further studied using PIL–PNIPAM block copolymers with varying PNIPAM chain lengths. The EOF mobility was measured in phosphate buffer (ionic strength of 20 mM) at pH 7.4 after a short pretreatment with a 0.5 mg/mL solution of the different block copolymers. The studies were carried out at 25 and 45 °C. The mobility values of the EOF marker (thiourea) are shown in Figure 4. At room temperature, the changes in the EOF mobility with a change in the length of the PNIPAM block were minor with RSD values between 0.2 and 2.3%. No obvious interactions between the diblock copolymer and the fused silica capillary wall occurred at room temperature.

Such weak interactions evidence that the polymeric micellar structure is neither electrostatically nor hydrophobically adsorbed onto the negatively charged fused silica wall. However, at 45 °C the EOF mobilities changed from cathodic to anodic owing to the profound changes in the structure of copolymer. The changes in the EOF mobility were observed with all studied diblock copolymers. This is most probably due to changes in the micellar structures. The EOF mobility was also at the higher temperature (45 °C) practically

constant with RSD values from 0.1 to 2.6%. These data demonstrate that CE is an efficient and easy method for fast screening of structural changes of such polymeric structures. The most crucial requirement is that the polarity (voltage) of the CE instrument can be altered from positive to negative.

The differences between the measurements done at 25 and 45 °C are due to the much higher zeta potential (higher electrophoretic mobility) of the particles at the latter temperature (Supporting Information Figure S6). All the polymer solutions show increasing zeta potential in phosphate buffer with increasing temperature, although the increase is less pronounced with the two longer block copolymers in pure water (Supporting Information Figure S7). This is due to the changes in particle structures (please see the discussion below), which leads to the formation of particles with PNIPAM cores and cationic PIL coronae.

3.4 | Asymmetrical flow-field flow fractionation of diblock copolymers

To further study the structural transformation of the copolymers, the effect of temperature on the copolymer structure was determined by AF4 at 25 and 45 °C. The studies were carried out on a regenerated cellulose separation membrane (molecular mass cut-off of 10 kDa) with an isoelectric point around 3.4, meaning that the membrane is negatively charged at pH values above 3.4 [40]. Therefore, at physiological conditions electrostatic interactions between the positively charged analytes (i.e., the studied polymers) and the negatively charged membrane surface lead to analyte adsorption [41]. To diminish the adsorption of cationic diblock copolymers, the separation membrane was first preconditioned with BSA, causing repulsive forces between the analytes and the positively charged separation membrane [42]. As shown in Figure 5, the overall elution profile of diblock copolymers could be detected. The baselines of PIL_{24}–$PNIPAM_{26}$ (Figure 5A and B) are slightly drifting, indicating some adsorption of the copolymer on the channel membrane surface. The adsorption was stronger at elevated temperature, probably due to an increase in the hydrophobicity and positive surface charge of the diblock copolymers. The fact that the elution profile of PIL_{24}–$PNIPAM_{26}$ remains relatively unchanged at the two studied temperatures is in line with the observation that no phase transition temperature could be observed for this copolymer.

A similar effect was observed for PIL_{24}–$PNIPAM_{14}$ and PIL_{24}–$PNIPAM_{59}$ diblock copolymers (data not shown), while, interestingly, in the case of PIL_{24}–$PNIPAM_{88}$ the formation of two fractions was observed (Figure 5E and F). Moreover, at higher temperature, the magnitude of the second fraction increased, which demonstrates profound changes in the associate structures.
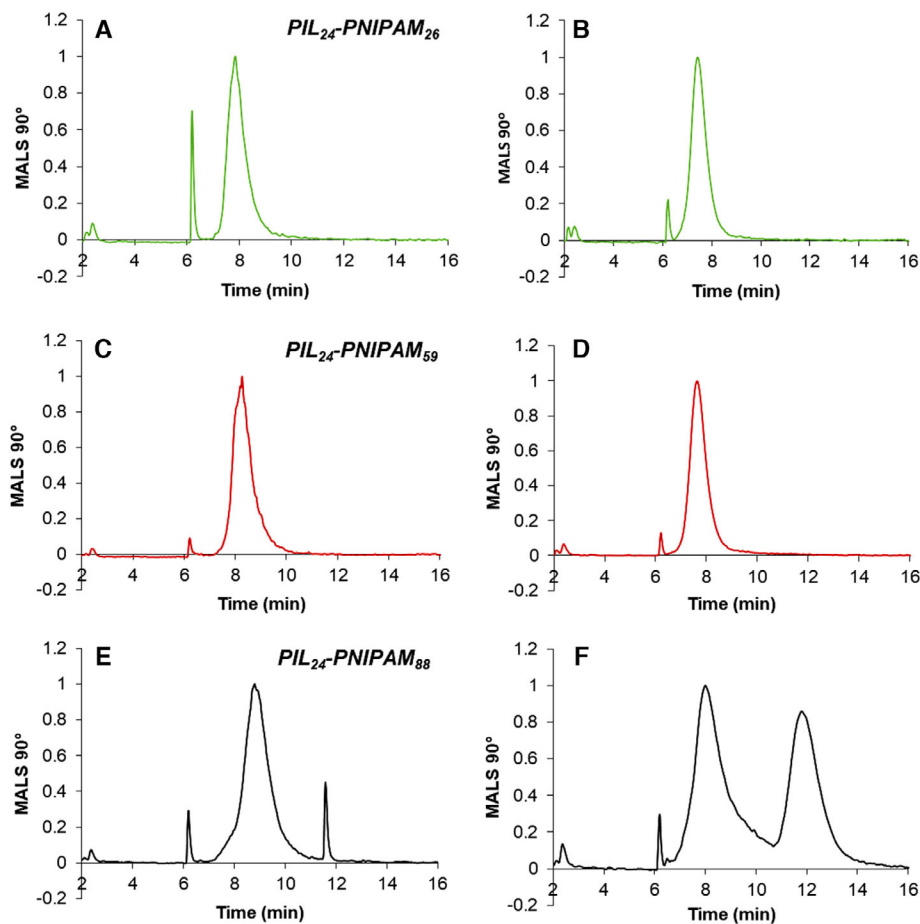
FIGURE 5 The effect of temperature on the PIL_{24}–$PNIPAM_{26}$ (green), PIL_{24}–$PNIPAM_{59}$ (red), and PIL_{24}–$PNIPAM_{88}$ (black) diblock copolymer structures. AF4 studies were carried out at 25 °C (A; C; E) and 45 °C (B; D; F). Running conditions: sodium phosphate buffer pH 7.4 (ionic strength of 20 mM) with 0.02% m/v sodium azide as carrier solution, injection volume 60 μL, detector flow rate 1.0 mL/min, injection at 0.2 mL/min with an injection time of 2 min, and the cross-flow rate at 1.7 mL/min. The copolymer concentrations were 1.0 mg/mL

The observation that neither of the two shorter block copolymers show any change in AF4 is explainable through their size distributions. The distributions measured at a scattering angle of 173° for PIL_{24}–$PNIPAM_{14}$ and PIL_{24}–$PNIPAM_{26}$ are very similar at 20 and 45 °C (Supporting Information Figures S8 and S9). This is in line with the intensity of the scattered light at 173° (Supporting Information Figure S10), which shows no significant increase for either of the aforementioned copolymers below 45 °C. This indicates that no phase transition takes place in this temperature range. When particles of the same block copolymers were made through solvent exchange from dimethyl formamide to water, no phase transition was observed either [18].

The two block copolymers with longer PNIPAM chains show a noticeable increase in scattering intensity and PIL_{24}–$PNIPAM_{88}$ shows bimodal distributions at both temperatures (Supporting Information Figure S11). Intensity average size distributions overemphasize the higher distributions, meaning that the larger of the two observed distributions is virtually nonexistent at 20 °C and the smaller is much more relevant

than it is obvious at 45 °C. This can be clearly seen when the distributions are presented at both temperatures as volume average values, assuming spherical particles (Supporting Information Figure S12), which are then seen in the AF4 measurement (Figure 5). The reader is advised to note that spherical particles might not be a valid assumption at both temperatures, but nevertheless it is a better indication about the "real" sizes of the formed particles than the intensity weighted one. For PIL_{24}–$PNIPAM_{59}$, the particles are different at 20 and 45 °C, which is clear from both intensity weighted (Supporting Information Figure S13) and volume-weighted distributions (Supporting Information Figure S14). Only one distribution is observed at 45 °C and this explains why only peak distribution is observed in the AF4 measurements for PIL_{24}–$PNIPAM_{59}$ (Figure 5D).

The reason behind the bimodal distribution observed for PIL_{24}–$PNIPAM_{88}$ at 45 °C in phosphate buffer seen both in light scattering (Supporting Information Figures S11 and S12) and AF4 (Figure 5) is that the phase transition is still incomplete at the studied temperature. This can be seen when

TABLE 1 Refractive indexes of PILs containing different lengths of PNIPAM blocks

Type of diblock copolymer	$\frac{dn}{dc}$ ($\frac{mL}{g}$)	R^2
PIL_{24}–$PNIPAM_{14}$	-0.0800 ± 0.0006	0.9998
PIL_{24}–$PNIPAM_{26}$	-0.0757 ± 0.0003	1.0000
PIL_{24}–$PNIPAM_{59}$	-0.0603 ± 0.0002	0.9999
PIL_{24}–$PNIPAM_{88}$	-0.0494 ± 0.0001	1.0000

measuring the intensity of scattered light as a function of temperature (Supporting Information Figure S10) as the scattering intensity has not leveled at 45 °C. After the intensity reaches a constant value, only one distribution is observed (Supporting Information Figures S15 and S16). The samples were heated very slowly (see experimental) so it is reasonable to assume that equilibrium structures are observed. Although the scattering intensity for PIL_{24}–$PNIPAM_{59}$ has not leveled at 45 °C (Supporting Information Figure S10), it shows only one distribution. It has been observed that for PIL–PNIPAM–PIL block copolymers, only a small change in the PIL/PNIPAM ratio results in radically different structures above the phase transition temperature [43]. Therefore, it is reasonable to assume that the polymers go through different transitional structures in this case as well. In addition, the nature of the final associate formed at high temperatures is probably very different between the two polymer, but this would be a subject of a study of its own and, thus, outside the scope of this article.

Subsequently, in order to determine the molar mass distribution, the refractive index of each diblock copolymer was measured applying batch mode in the concentration range of 0.1-0.9 mg/mL. However, as shown in Table 1, the dn/dc values are negative, preventing determination of the molar mass. This may be attributed to the presence of solvent remaining after dialysis or absorption of carbon dioxide to the diblock copolymers. The CE analysis did not reveal the presence of solvents, thus, the probable cause for the negative response is carbon dioxide adsorption, as the PIL is known to absorb CO_2 from air [44]. Nevertheless, the AF4 results clearly demonstrate that the temperature affects the structures of the polymer associates, resulting in their slight adsorption on the channel membrane, followed by the occurrence of aggregates. This is in a good agreement with the light scattering results.

3.5 | Interactions between diblock polymers and small analytes studied by EKC

The profound changes in the structure of the polymeric micelles could also result in the formation of aggregates with water insoluble cores capable of interacting with small nonpolar analytes. Therefore, neutral steroids and alkyl benzoates, were used as model compounds for evaluating
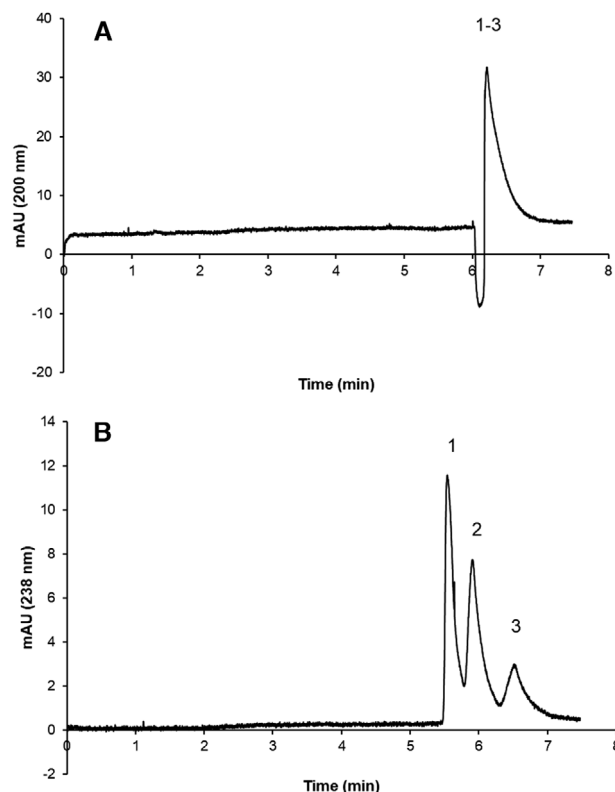

FIGURE 6 The effect of temperature on the EKC separation of steroids. The separations were carried out at 25 °C (A) and at 45 °C (B). The BGE was sodium phosphate buffer pH 7.4 (ionic strength of 20 mM) with 0.5 mg/mL of PIL_{24}–$PNIPAM_{88}$ diblock copolymer. Running conditions: ±25 kV, injection for 3 s at 50 mbar, L_{tot} 48.5 cm, L_{det} 40 cm, UV-detection at 200 and 238 nm, 0.5 mM thiourea as an EOF mobility marker. Peak numbering: (1) thiourea; (2) testosterone, and (3) progesterone. The concentrations of the steroids were 0.1 mg/mL

the capability the diblock copolymers containing different lengths of the PNIPAM block to take up these compounds. At this point, the aim was to investigate if the hydrophobicity of such diblock copolymers can be characterized by means of employing them as a pseudostationary phase in EKC. To study the effect of the length of the diblock copolymer, the same series of PIL block copolymers with varying PNIPAM block length ($n = 14$; 26; 59; or 88) were used.

First, the separation of neutral steroids was carried out at 25 and 45 °C in the presence of copolymers. The electropherograms of the separation with PIL_{24}–$PNIPAM_{88}$ copolymer electrolyte solution at both temperatures are presented in Figure 6. As expected, there were no interactions between the analytes and the copolymer BGE solutions studied at room temperature. However, a substantial delay in the mobility of the EOF marker and the steroids could be observed when the copolymer was included in the BGE solution. This was most probably due to a small increase in the viscosity of the solution. At elevated temperatures, positively charged
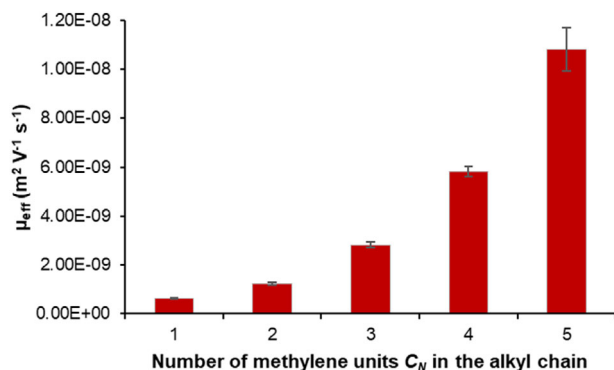
FIGURE 7 Effective electrophoretic mobility against the methylene number (C_N) of the alkyl group of a homologous series of alkyl benzoates using sodium phosphate pH 7.4 (ionic strength of 20 mM) with 0.5 mg/mL of PIL$_{24}$–PNIPAM$_{59}$ diblock copolymer BGE solution at 45 °C. Running conditions: –25 kV, injection for 3 s at 50 mbar, L_{tot} 48.5 cm, L_{det} 40 cm, UV-detection at 200 nm. Analytes: 0.5 mM thiourea as an EOF mobility marker and 0.1 mg/mL of alkyl benzoates in sodium phosphate pH 7.4 (ionic strength of 20 mM)

aggregates form (Supporting Information Figure S6). As shown in Figure 6, successful separation of the neutral steroids was obtained at 45 °C. The separation was only possible when PIL$_{24}$–PNIPAM$_{59}$ and PIL$_{24}$–PNIPAM$_{88}$ were added to the running buffer. No separation of the steroids was observed using PIL$_{24}$–PNIPAM$_{14}$ or PIL$_{24}$–PNIPAM$_{26}$ in the CE BGE solution. This is explainable by the fact that no clear phase transition is observed for the two shorter block copolymers (Supporting Information Figure S10), so no hydrophobic microenvironment is formed at 45 °C. The zeta potential of the two shorter blocks increases with increasing temperature (Supporting Information Figure S6), which could be caused by changes in solubility of the PIL block (please see discussion above). This change in surface charge explains the observed change of EOF between the two measurement temperatures.

To further study the observation that the cationic copolymer micelles can interact with small neutral analytes, EKC studies on alkyl benzoates were carried out. Again, the separation was performed in the presence of copolymers at 25 and 45 °C. Our results showed no interaction between alkyl benzoates and the copolymer BGE solutions studied at room temperature. Successful separation of the alkyl benzoates (methyl, ethyl, propyl, butyl, and pentyl benzoates) was only possible when PIL$_{24}$–PNIPAM$_{59}$ was utilized in the running buffer studied at elevated temperature. The effective mobilities of the alkyl benzoates increased with the number of methylene groups in the alkyl chain using PIL$_{24}$–PNIPAM$_{59}$ diblock copolymer in sodium phosphate pH 7.4 (ionic strength of 20 mM) as BGE solution (Figure 7). There was no separation of the alkyl benzoates using PIL$_{24}$–PNIPAM$_{88}$ in the BGE solution. Again, the reason for the dif-

ferences in copolymer properties is related to the length of the PNIPAM block copolymers. However, the reason for the unsuccessful separation using PIL$_{24}$–PNIPAM$_{88}$ in the BGE solution is unclear, however, one possible explanation is the considerable difference in the hydrophobicity between PIL$_{24}$–PNIPAM$_{59}$ and PIL$_{24}$–PNIPAM$_{88}$. Nevertheless, it can be concluded that PIL$_{24}$–PNIPAM$_{59}$ experienced the most profound changes in its hydrophobic properties.

Of particular interest was also to find out whether the concentration of the diblock copolymers could enhance the separation of the compounds. The separations were carried out at 45 °C with PIL$_{24}$–PNIPAM$_{59}$ and PIL$_{24}$–PNIPAM$_{88}$ copolymer BGE solutions in the concentration range of 0.1 to 0.5 mg/mL. The separation was still successful when a higher copolymer concentration was employed, however, there were no improvements in the separation efficiency or selectivity of the compounds (data not shown).

4 | CONCLUDING REMARKS

Thermoresponsive diblock copolymers based on a hydrophobic PIL block and an amphiphilic PNIPAM one with a varying degree of polymerization of the PNIPAM block form micellar structures in aqueous solvents. These polymers were investigated by capillary electrophoresis and AF4. To get information on the structural/conformational changes of the copolymers, the measurements were carried out below and above their phase transition temperatures. The obtained results showed profound changes in the polymer assemblies. Diblock copolymers generated a reversed and stable electroosmotic flow mobility at elevated temperature due to the thermal collapse of the PNIPAM blocks. The AF4 results supported the structure transformation of the PIL–PNIPAM diblock copolymers leading to their adsorption on the separation channel membrane. Moreover, our studies demonstrate the applicability of electrokinetic capillary chromatography to the characterization of such copolymers, by using them as pseudostationary phase for the separation of neutral water-insoluble compounds. The analyte migration times were overlapping at room temperature, but they were successfully separated using the longest blocks of PNIPAM at elevated temperature. The results show that CE and AF4 are complimentary methods that are well suited for the characterization of such diblock copolymers.

CONFLICT OF INTEREST

The authors have declared no conflict of interest.

ORCID

Joanna Witos (ID) https://orcid.org/0000-0003-0021-1599
Erno Karjalainen (ID)
https://orcid.org/0000-0001-9247-813X
Heikki Tenhu (ID) https://orcid.org/0000-0001-5957-4541
Susanne K. Wiedmer (ID)
https://orcid.org/0000-0002-3097-6165

REFERENCES

1. Yuk, S. H., Bae, Y. H., Phase-transition polymers for drug delivery. *Crit. Rev.*ᵀᴹ *Therap. Drug Carrier Syst.* 1999, *16*, 385–423.
2. Wiedmer, S. K., Riekkola, M. L., Tenhu, H., Interactions of diuretics with a neutral temperature-responsive polymer: Study by capillary electrophoresis and dynamic light scattering. *J. Capill. Electrophor. Microchip. Technol.* 1999, *6*, 163–168.
3. Pelton, R., Poly (*N*-isopropylacrylamide)(PNIPAM) is never hydrophobic. *J. Colloid Interface Sci.* 2010, *348*, 673–674.
4. Yamauchi, H., Maeda, Y., LCST and UCST behavior of poly (*N*-isopropylacrylamide) in DMSO/water mixed solvents studied by IR and micro-Raman spectroscopy. *J. Phys. Chem. B.* 2007, *111*, 12964–12968.
5. Marcilla, R., Sanchez-Paniagua, M., Lopez-Ruiz, B., Lopez-Cabarcos, E., Ochoteco, E., Synthesis and characterization of new polymeric ionic liquid microgels. *J. Polym. Sci. Pol. Chem.* 2006, *44*, 3958–3965.
6. Muldoon, M. J., Gordon, C. M., Synthesis of gel-type polymer beads from ionic liquid monomers. *J. Polym. Sci. Pol. Chem.* 2004, *42*, 3865–3869.
7. Tsioptsias, C., Panayiotou, C., Preparation of cellulose-nanohydroxyapatite composite scaffolds from ionic liquid solutions. *Carbohydr. Polym.* 2008, *74*, 99–105.
8. Green, O., Grubjesic, S., Lee, S., Firestone, M. A., The design of polymeric ionic liquids for the preparation of functional materials. *Polym. Rev.* 2009, *49*, 339–360.
9. Sayin, S., Ozdemir, E., Acar, E., Ince, G. O., Multifunctional one-dimensional polymeric nanostructures for drug delivery and biosensor applications. *Nanotechnology* 2019, *30*, 412001.
10. Mabape, K., Donga, C., Mishra, S., Mishra, A., Smart Polymer Catalysts and Tunable Catalysis. Elsevier Amsterdam 2019, pp. 77–94.
11. Hosseini, M. S., Amjadi, I., Mohajeri, M., Iqbal, M. Z., Wu, A., Mozari, M., Advanced Functional Polymers for Biomedical Applications. Elsevier Amsterdam 2019, pp. 301–322.
12. Rogers, R. D., Seddon, K. R., Chemistry. Ionic liquids–solvents of the future? *Science* 2003, *302*, 792–793.
13. Parviainen, A., King, A. W., Mutikainen, I., Hummel, M., Selg, C., Predicting cellulose solvating capabilities of acid–base conjugate ionic liquids. *ChemSusChem* 2013, *6*, 2161–2169.
14. Holding, A. J., Heikkilä, M., Kilpeläinen, I., King, A. W., Amphiphilic and phase-separable ionic liquids for biomass processing. *ChemSusChem* 2014, *7*, 1422–1434.
15. Hummel, M., Michud, A., Tanttu, M., Asaadi, S., Ma, Y., Hauru, L. K. J., Parviainen, A., King, A. W. T, Kilpeläinen, I., Sixta, H., *Cellulose Chemistry and Properties*: *Fibers, Nanocelluloses and Advanced Materials*. Springer New York 2015, pp. 133–168.
16. Sun, P., Armstrong, D. W., Ionic liquids in analytical chemistry. *Anal. Chim. Acta* 2010, *661*, 1–16.
17. Muhammad, N., Man, Z., Khalil, M. A. B., Ionic liquid—A future solvent for the enhanced uses of wood biomass. *Eur. J. Wood Wood Prod.* 2012, *70*, 125–133.
18. Karjalainen, E., Chenna, N., Laurinmäki, P., Butcher, S. J., Tenhu, H., Diblock copolymers consisting of a polymerized ionic liquid and poly (*N*-isopropylacrylamide). Effects of PNIPAM block length and counter ion on self-assembling and thermal properties. *Polym. Chem.* 2013, *4*, 1014–1024.
19. Fraser, K. J., MacFarlane, D. R., Phosphonium-based ionic liquids: An overview. *Aust. J. Chem.* 2009, *62*, 309–321.
20. Yuan, J., Antonietti, M., Poly (ionic liquid) s: Polymers expanding classical property profiles. *Polymer* 2011, *52*, 1469–1482.
21. Huang, Y., Yao, S., Song, H., Application of ionic liquids in liquid chromatography and electrodriven separation. *J. Chromatogr. Sci.* 2013, *51*, 739–752.
22. Duša, F., Witos, J., Karjalainen, E., Viitala, T., Tenhu, H., Novel cationic polyelectrolyte coatings for capillary electrophoresis. *Electrophoresis* 2016, *37*, 363–371.
23. Lokajová, J., Railila, A., King, A. W., Wiedmer, S. K., Determination of the distribution constants of aromatic compounds and steroids in biphasic micellar phosphonium ionic liquid/aqueous buffer systems by capillary electrokinetic chromatography. *J. Chromatogr. A* 2013, *1308*, 144–151.
24. Tang, S., Liu, S., Guo, Y., Liu, X., Jiang, S., Recent advances of ionic liquids and polymeric ionic liquids in capillary electrophoresis and capillary electrochromatography. *J. Chromatogr. A* 2014, *1357*, 147–157.
25. Berthod, A., Ruiz-Ángel, M., Carda-Broch, S., Recent advances on ionic liquid uses in separation techniques. *J. Chromatogr. A* 2018, *1559*, 2–16.
26. Zhang, Q., Ionic liquids in capillary electrophoresis for enantioseparation. *Trends Anal. Chem.* 2018, *100*, 145–154.
27. Yohannes, G., Sneck, M., Varjo, S. J., Jussila, M., Wiedmer, S. K., Miniaturization of asymmetrical flow field-flow fractionation and application to studies on lipoprotein aggregation and fusion. *Anal. Biochem.* 2006, *354*, 255–265.
28. Yohannes, G., Pystynen, K., Riekkola, M. L., Wiedmer, S. K., Stability of phospholipid vesicles studied by asymmetrical flow field-flow fractionation and capillary electrophoresis. *Anal. Chim. Acta* 2006, *560*, 50–56.
29. Yohannes, G., Jussila, M., Hartonen, K., Riekkola, M., Asymmetrical flow field-flow fractionation technique for separation and characterization of biopolymers and bioparticles. *J. Chromatogr. A* 2011, *1218*, 4104–4116.
30. Witos, J., Cilpa, G., Yohannes, G., Öörni, K., Kovanen, P. T., Sugar treatment of human lipoprotein particles and their separation by capillary electrophoresis. *J. Sep. Sci.* 2010, *33*, 2528–2535.
31. Marcilla, R., Alberto Blazquez, J., Rodriguez, J., Pomposo, J. A., Mecerreyes, D., Tuning the solubility of polymerized ionic liquids by simple anion-exchange reactions. *J. Polym. Sci. Pol. Chem.* 2004, *42*, 208–212.
32. Marcilla, R., Blazquez, J. A., Fernandez, R., Grande, H., Pomposo, J. A., Synthesis of novel polycations using the chemistry of ionic liquids. *Macromol. Chem. Phys.* 2005, *206*, 299–304.

33. Karjalainen, E., Aseyev, V., Tenhu, H., Counterion-induced UCST for polycations. *Macromolecules* 2014, *47*, 7581–7587.

34. Karjalainen, E., Aseyev, V., Tenhu, H., Upper or lower critical solution temperature, or both? Studies on cationic copolymers of *N*-isopropylacrylamide. *Polym. Chem.* 2015, *6*, 3074–3082.

35. Zhang, Y., Furyk, S., Bergbreiter, D. E., Cremer, P. S., Specific ion effects on the water solubility of macromolecules: PNIPAM and the Hofmeister series. *J. Am. Chem. Soc.* 2005, *127*, 14505–14510.

36. Kujawa, P., Segui, F., Shaban, S., Diab, C., Okada, Y., Impact of end-group association and main-chain hydration on the thermosensitive properties of hydrophobically modified telechelic poly (*N*-isopropylacrylamides) in water. *Macromolecules* 2006, *39*, 341–348.

37. Xia, Y., Burke, N. A., Stöver, H. D., End group effect on the thermal response of narrow-disperse poly (*N*-isopropylacrylamide) prepared by atom transfer radical polymerization. *Macromolecules* 2006, *39*, 2275–2283.

38. Chung, J., Yokoyama, M., Suzuki, K., Aoyagi, T., Sakurai, Y., Reversibly thermo-responsive alkyl-terminated poly (*N*-isopropylacrylamide) core-shell micellar structures. *Colloids Surf. B.* 1997, *9*, 37–48.

39. Nuopponen, M., Ojala, J., Tenhu, H., Aggregation behaviour of well defined amphiphilic diblock copolymers with poly (*N*-isopropylacrylamide) and hydrophobic blocks. *Polymer* 2004, *45*, 3643–3650.

40. Lee, S., Kwen, H. D., Lee, S. K., Nehete, S. V., Study on elution behavior of poly (amidoamine) dendrimers and their interaction with bovine serum albumin in asymmetrical flow field-flow fractionation. *Anal. Bioanal. Chem.* 2010, *396*, 1581–1588.

41. Wagner, M., Pietsch, C., Tauhardt, L., Schallon, A., Schubert, U. S., Characterization of cationic polymers by asymmetric flow field-flow fractionation and multi-angle light scattering—A comparison with traditional techniques. *J. Chromatogr. A* 2014, *1325*, 195–203.

42. Ulrich, A., Losert, S., Bendixen, N., Al-Kattan, A., Hagendorfer, H., Critical aspects of sample handling for direct nanoparticle analysis and analytical challenges using asymmetric field flow fractionation in a multi-detector approach. *J. Anal. At. Spectrom.* 2012, *27*, 1120–1130.

43. Karjalainen, E., Khlebnikov, V., Korpi, A., Hirvonen, S., Hietala, S., Complex interactions in aqueous PIL—PNIPAm—PIL triblock copolymer solutions. *Polymer* 2015, *58*, 180–188.

44. Privalova, E. I., Karjalainen, E., Nurmi, M., Mäki-Arvela, P., Eränen, K., Imidazolium-based poly (ionic liquid) s as new alternatives for CO_2 capture. *ChemSusChem* 2013, *6*, 1500–1509.

SUPPORTING INFORMATION

Additional supporting information may be found online in the Supporting Information section at the end of the article.